Contact-Induced Structure Transformation in Transmembrane Prion Propagation

D.-M. Ou, C.-C. Chen, and C.-M. Chen
Department of Physics, National Taiwan Normal University, Taipei, Taiwan

ABSTRACT Based on recent experimental evidences of the transmission of prion diseases due to a particular transmembrane form (termed ^{Ctm}PrP), we propose a theoretical model for the molecular mechanism of such conformational diseases, in which a misfolded ^{Ctm}PrP induces a similar misfolding of another ^{Ctm}PrP. Computer simulations are performed to investigate the correlation between folding time and the concentration of misfolded PrP in various processes, including dimerization, trimerization, and cooperative dimerization. By comparing with the experimental correlation curve between incubation time and injected dose of scrapie prions, we conclude that cooperative dimerization may play an important role in the pathological mechanism of prion diseases.

INTRODUCTION

Prion diseases, such as scrapie, bovine spongiform encephalopathy, Creutzfeldt-Jakob disease, and Gerstmann-Straussler-Scheinker disease, are fatal neurodegenerative disorders characterized by dementia, ataxia, and cerebral spongiosis (1–5). They constitute a heterogeneous group of infectious, sporadic, and inheritable conditions, which are now believed to be due to conformational conversion of a normal brain prion protein called PrP^{c} to a protease-resistant isoform denoted PrP^{Sc}. Based on the correlation between the accumulation of PrP^{Sc} and the degree of neuronal damage during the course of prion diseases, it is often assumed that this isoform is the main cause of neurodegeneration.

The role of PrP^{Sc} in the pathologic mechanism of prion diseases is currently unknown. Recent experiments have observed that PrP^{Sc} deposition fails to cause disease in brain tissue lacking PrP^{c} and that the time course of PrP^{Sc} deposition in the brains of mice expressing low levels of PrP^{c} does not correlate with the time course of neurodegeneration (6,7). Conversely, it is also observed that substantial neurodegeneration could occur in the absence of PrP^{Sc} accumulation in several prion diseases (8–12). These observations suggest that PrP^{Sc} is not directly toxic and its accumulation is not the only cause of pathology in prion diseases.

Studies of PrP translocation at the endoplasmic reticulum (ER) membrane have found three topologic forms of PrP, including one cell-surface form (^{sec}PrP) and two transmembrane (TM) forms (^{Ctm}PrP and ^{Ntm}PrP) (13–15). Several pieces of evidence have implied the importance of ^{Ctm}PrP in the pathogenesis of prion diseases. It is found that transgenic mice overexpressing ^{Ctm}PrP develop a spontaneous neurological disease with scrapie-like features, in the absence of PrP^{Sc}. In addition, patients affected by Gerstmann-Straussler-Scheinker disease associated to an A117V mutation exhibit an increased production of this TM form of PrP, suggesting that the basis of this disease lies in increased production of ^{Ctm}PrP (16,17). These findings suggest that ^{Ctm}PrP may have important implications for a broad range of neurodegenerative diseases. Nevertheless, not much is known about the pathological mechanism so far.

Numerous computational studies have provided valuable information about the structure and mechanism of formation of amyloids by using various modeling techniques and various levels of protein representation (18–22). Simulations at the atomic resolution can study relative stability and flexibility of the native structure of prions, their amyloidlike model structure, and possible intermediate structures during aggregation (19,20). However, it would be computationally too demanding to investigate protein refolding and aggregation. On the other hand, idealized simple lattice models have shown that prion aggregation can lead to significant change of the single chain conformation (21). Moreover, simulations at protein level can provide a bridge between the short distance and timescales covered in individual protein models and the long time, macroscopic realm of chemical kinetics (22).

In this work, we propose a model for the contact-induced structure transformation of the transmembrane domain of ^{Ctm}PrP, which is studied by Monte Carlo simulations using a coarse-grained protein model. In this model, the transmembrane domain can fold into a well-defined helical ''native conformation'' (Fig. 1 *a*) and also assume a metastable β-type structure (Fig. 1 *b*). For a protein monomer, the helical structure corresponds to the global energy minimum and the metastable structure to a higher-energy local minimum of the energy landscape. For a system of more than one chain, the ground state structure of the energy landscape is a linear crystal consisting of β-form chains. Similar mechanisms have been previously proposed for a prionlike propagation in solution using a lattice model (23,24) or an off-lattice reduced protein model (20), whose purpose is to mimic the observed amyloid aggregation in solution with

Submitted September 28, 2006, and accepted for publication January 9, 2007.

Address reprint requests to C.-M. Chen, E-mail: cchen@phy.ntnu.edu.tw.

0006-3495/07/04/2704/07 $2.00

doi: 10.1529/biophysj.106.098335

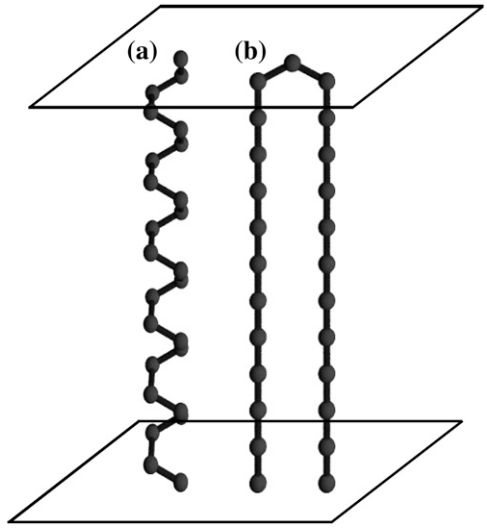

FIGURE 1 The native α-helical conformation (*a*) and the metastable β-hairpin conformation (*b*) of the amino-acid sequence HMAGAAAAGA VVGGLGGYML GSAMV.

certain artificially designed amino-acid sequences. In this article, we investigate the problem of prion propagation for the transmembrane domain of ^{Ctm}PrP, which infers a new perspective of the pathological mechanism of prion diseases as suggested by recent experiments (13–17). We speculate that the amyloid aggregation in the membrane could lead to rupture of membrane and cause the death of nerve cells. This model is used to investigate the correlation between concentration and the average refolding time of a helical form to a β-form, in the presence of a β-form template. We find that cooperativity plays an important role in the contact-induced structure transformation. In this case, an excellent agreement with experimental data for transgenic mice is found in the calculated correlation between folding time and prion concentration (25).

MODEL

In our model, the potential energy U of a membrane protein (MP) can be expressed as $U = U_{\text{membrane}} + U_{\text{water}}$, where U_{membrane} and U_{water} are the potential energies of MPs in a membrane and in water, respectively (26). The simulation box is divided into three regions including two water phases separated by a hydrocarbon (membrane) phase of thickness L. For amino acids within the membrane, their potential energy is given by $U_{\text{membrane}} = E_{\text{H-bond}} + E_{\text{bend}}$, where $E_{\text{H-bond}}$ is the hydrogen-bonding energy and E_{bend} is the bending energy of the chain. A hydrogen bond can form if two amino acids are separated by four-lattice spacing (or 5.4 Å). However, each amino acid can, at most, participate in two hydrogen bonds. Moreover, hydrogen bonding is highly directional and has a maximal strength when N-H and O=C bonds are co-linear. Therefore we model the hydrogen-bonding energy by $E_{\text{H-bond}} = \sum_{\langle i,j\rangle} |(n_i \cdot r_{ij})\,(n_j \cdot r_{ij})|\,\delta_{r(i,j),4}$, where n_i is the N-H (or O=C) bond orientation of the i^{th} amino acid, while $r(i,j)$ and r_{ij} are the distance and its unit vector between amino acids i and j. Since the backbone hydrogen bonding is the dominant interaction for the formation of secondary structures of MPs, its energy strength is set to unity. Furthermore we have explicitly excluded the possibility of forming 2_7 ribbons and 3_{10} helices due to steric hindering by disallowing the hydrogen bonding between (i, $i\pm2$) and (i, $i\pm3$) pairs. The bending energy of the chain is assumed to be $e_1 \sum_i (1-\cos\theta_i)$, where e_1 is the bending rigidity and θ_i is the angle between two consecutive bonds i and $i+1$. For amino acids in water, their interactions are modeled by a residue-residue contact potential (E_{contact}) and the hydropathical interaction ($E_{\text{hydropathy}}$), i.e., $U_{\text{water}} = E_{\text{contact}} + E_{\text{hydropathy}}$. The interactions between the exposed residues and the lipid bilayer are ignored. Here we use the Thomas-Dill contact potential with strength e_2 to model the residue-residue interaction in water when residues are in contact (27). Since MP residues exposed to water are mostly exterior residues, the positive contact energies between exterior residues in this potential imply highly dynamical loops of MPs in the water phase. The hydropathical interaction of amino acids in water can be modeled by using a rescaled Hopp-Woods hydropathy index [A, R, N, D, C, E, Q, G, H, I, L, K, M, F, P, S, T, W, Y, V] = [0.15, −0.88, −0.06, −0.88, 0.29, −0.06, −0.88, 0, 0.15, 0.53, 0.53, −0.88, 0.38, 0.74, 0, −0.09, 0.12, 1, 0.68, 0.44] with strength e_3, which is mainly determined by the Gibbs free energy change for transferring amino acids from water into condensed vapor (28). In addition, the insertion of a polypeptide chain into a membrane will disturb the integrity of the membrane and local lipid density around the chain, which increases the energy of the membrane (29). We model this effect by introducing an effective lateral pressure (P) applied to the polypeptide chain to minimize its lateral area A (30). Therefore, to find the ground state structure of MPs, the relevant physical quantity to be minimized in our model is the enthalpy $H = U + PA$. In our simulations, the parameters of this model are chosen to be $e_1 = 0.016$, $e_2 = 0.3$, $e_3 = 0.66$, $P = 0.59$, and $L = 26$, in which case the unique ground state is a transmembrane helix for a single protein system but is a linear hairpin aggregation for a multiprotein system. In this set of parameters, we deliberately set the energy of a hairpin dimer to be only slighter lower than that of two isolated helices. We have previously found that, for a protein monomer, it is kinetically unfavorable to find the state of a hairpin structure due to the required nonlocal interaction (30). In fact, only $<4\%$ of our simulations will reach the hairpin state and the helical state is found in most simulations. In the presence of a hairpin template, the kinetic barrier disappears due to the interaction between protein monomer and the template. It is easy to see the propagation of β-hairpins even with the current set of parameters. If a different set of parameters is chosen, such as using a larger value of e_1, the aggregation of β-hairpins will be further stabilized and the propagation of β-hairpins will be more prominent. In the absence of a hairpin template, we have never seen the transition from two isolated helices into a hairpin dimer.

Algorithm of simulations

Protein is represented as a chain of monomers in lattice space using the bond fluctuation model (31). Each monomer in the model is a cube of length 1 (lattice spacing) on a cubic lattice. The set of allowed bond vectors is B = P(2,0,0)∪P(2,1,0)∪P(2,1,1)∪P(2,2,1)∪P(3,0,0)∪P(3,1,0), where P(a,b,c) stands for the set of all permutations and sign combinations of $\pm a$, $\pm b$, $\pm c$. The number of configurations per bond is $z = 108$. The length of one bond can take any one of the five values: 2, $5^{1/2}$, $6^{1/2}$, 3, or $10^{1/2}$ (in units of lattice spacing). Chains satisfy the excluded volume constraint: no lattice site may be occupied by more than one monomer. The set B is chosen to satisfy the constraints of both excluded volume between monomers and topological entanglement between chains (i.e., two chains cannot pass through each other). If any other bond vectors were added to this set, some chains would become ''phantom'' chains. The folding of a protein chain is simulated by the Metropolis Monte Carlo (MC) algorithm in a cubic lattice at a constant temperature T. At each instant, a residue is picked up at random and attempts to move in any of the six directions by one lattice spacing. If any attempted move of residues satisfies the excluded volume constraint and the new bond vectors are still in the allowed set, then the move is accepted with probability $p = \min[1, \exp(-\Delta H/T)]$, where ΔH is the enthalpy change of the system. Each physical quantity calculated in the present work is averaged over 100 different runs.

RESULTS AND DISCUSSION

In Fig. 2, we display the average hydropathy index of a S135V mutated Syrian hamster prion protein ($SHaPrP^{29–231}$, GG WNTGGSRYPG QGSPGGNRYP PQGGGTWGQP HGGGWGQPHG GGWGQPHGGG WGQPHGGGWG QGGGTHNQWN KPSKPKTNMK HMAGAAAAGA VVGGLGGYML GSAMVRPMMH FGNDWEDRYY RENMNRYPNQ VYYRPVDQYN NQNNFVHDCV NITIKQHTVT TTTKGENFTE TDIKIMERVV EQMCTT-QYQK ESQAYYDGRR S) for window sizes (WS) of 20, 24, and 25 residues. Our calculation on the average hydropathy index for WS = 20 ~ 30 residues shows that ShaPrP contains a stable TM domain stretching from H^{111} to V^{135}, which has the largest accumulated hydropathy index ($\Delta E^{111-135}_{\text{hydropathy}} = 5.28$) for various values of WS. Similar TM domain (stretching from M^{112} to V^{135}) is predicted if the Hoop-Woods index is replaced by the Kyte-Doolittle index, as shown in Fig. 3. In our model, the native conformation of this TM domain corresponds to the structure of a simple α-helical motif (Fig. 1 *a*), whereas the metastable structure adopted a β-motif (Fig. 1 *b*). The conformational energies of these structures are -13.9 and -8, respectively. With low-temperature range ($T = 0.1$–0.15) and the β-form as the initial configuration, the protein remains in the β-form for simulations of 10^6 MC steps, confirming its metastable character. Fig. 4 shows the temperature dependence of helical fraction and the mean first passage time (MFPT) to the helical state (ground state), starting from a random initial configuration. The optimal folding temperature for our model is 0.31 (the corresponding thermal energy is ~3 kJ/mol). The average helical fraction of the chain is calculated during a period of 10^3 MC steps for 10 different simulations at each temperature, after the chain has been simulated for 10^5 MC steps. The large values of helical fraction of the chain at various temperatures imply that there is a large basin associated with the helical state in the configuration space.

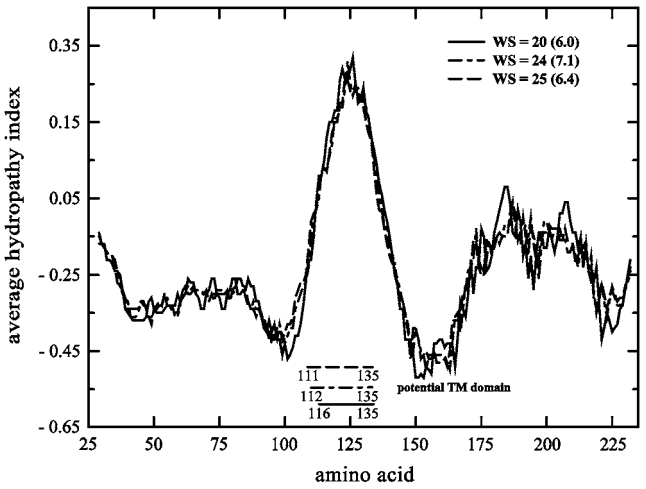

FIGURE 3 Average hydropathy index of S135V mutated Syrian hamster prion protein ($SHaPrP^{29–231}$) for WS = 20, 24, and 25 using the Kite-Doolittle hydropathy index. The predicted TM domain is also shown for these three values of WS.

Then, a system of two interacting protein molecules has been considered at $T = 0.31$. One of the molecules has been frozen in the β-form serving as a template. Such a frozen template may happen in real systems for various reasons (20,32). For example, this frozen template could be considered as a stable protein structure at the edge of a propagating amyloid rod. The initial configuration of the other protein is the α-helical motif, which is free to diffuse in the membrane. The α-helical form first unfolds and then refolds to the β-form in the presence of the template, assembling into a larger β-type dimer structure (Fig. 5). Due to the favorable intermolecule hydrogen bonding interaction, the energy of

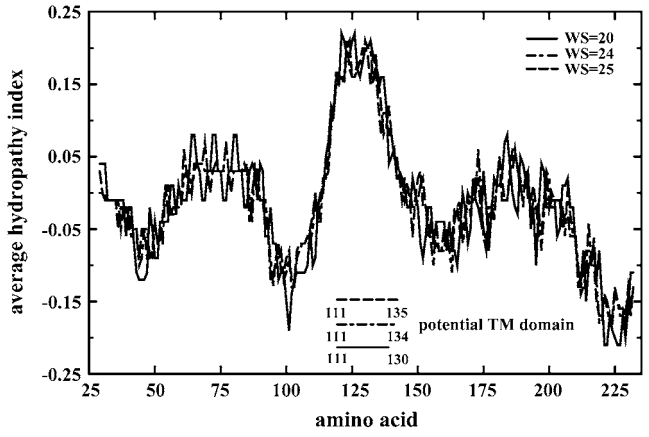

FIGURE 2 Average hydropathy index of S135V mutated Syrian hamster prion protein ($SHaPrP^{29-231}$) for WS = 20, 24, and 25 using the Hopp-Woods hydropathy index. The predicted TM domain is also shown for these three values of WS.

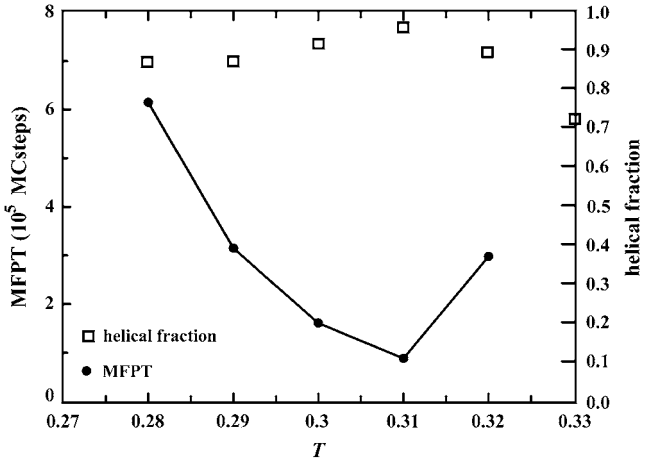

FIGURE 4 Temperature dependence of the chain's helical fraction and MFPT to the ground state for the amino-acid sequence HMAGAAAAGA VVGGLGGYML GSAMV, starting from a random initial configuration.

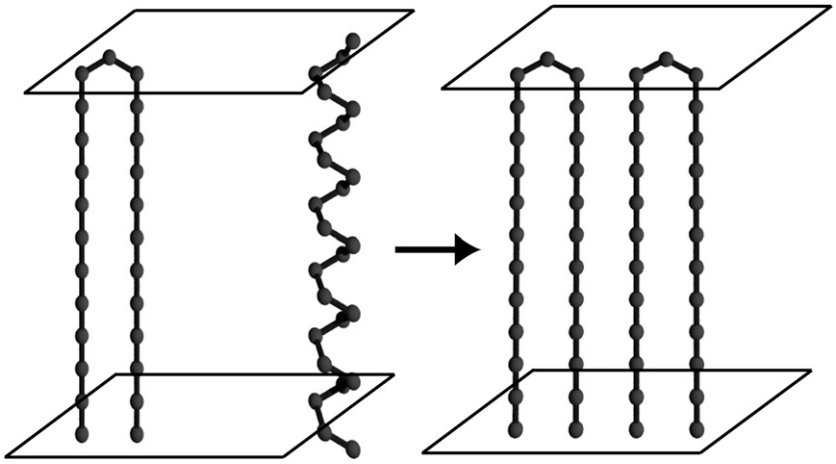

FIGURE 5 A model of prion disease propagation. The native helical form of a prion misfolds to a β-structure in the presence of the stiff misfolded β-structure form.

the dimer (-28) is lower than twice of the single-helical molecule (-27.8). If we use a random initial configuration for the second protein, it will quickly fold into the β-form due to its contact with the template. Such a dimer structure is stable for simulations longer than 10^6 MC steps at the optimal folding temperature, in which case both proteins are free to move. Nevertheless, the formation of the β-type dimer has never been observed in our simulations (longer than 10^7 MC steps) for systems starting from two unfolded or helical structures, which implies that a spontaneous transition from the native to the propagating scrapie form of the TM domain must be a rare event in our model. In this model, the hairpin structure is kinetically unfavorable due to the fact that hydrogen bonding is a local interaction for the helical state but is a nonlocal interaction for the hairpin state. As shown in Chen (30), only $<4\%$ of simulations will find a (twisted) hairpin state before the chain folds into a helical state, even when the (twisted) hairpin state is the ground state. This kinetic barrier will prevent the chain from folding into the hairpin structure in the absence of a hairpin template. In the presence of a hairpin template, the kinetic barrier no longer exists since proper contacts between monomer and template can facilitate the formation of dimers.

Dimerization in the β-form could be considered as an initiation event for a further propagation of an amyloid. Although the deposition of amyloid fibrils are often observed in most prion diseases, recent experiments have suggested that amyloid oligomers and protofibrils may actually be the toxic agents (33,34). We have also investigated the trimerization process in which initially one molecule is frozen in the β-form, and the other two freely moving molecules are either both helical or one helical and one β-type. In all cases, the resulting structure is a regular trimer composed of three TM β-hairpins, as shown in Fig. 6.

The correlations between MFPT and the concentration (C) of misfolded prions for dimerization (*open squares*) and trimerization (*open diamonds*) are compared to the experimental correlation curve between incubation time and injected dose of Sc237 prions into transgenic mice (25), as shown in Fig. 7. For the experimental curve, the injected dose decreases with incubation time as a power law with an exponent of -1.6. There seem to be two distinct phases for the disease incubation after inoculation: a lag phase during which there is little or no infectivity, and a doubling phase during which the infectivity increases exponentially (35–37). Since the lag phase period is much longer than the doubling phase period and the time spent in the doubling phase does not change appreciably with dose, here we approximate the incubation time by the lag phase time. Note that in this article we make no connection to the exponential growth of infectivity during the incubation period, which is due to our limited computing resources. In principle, as fibrils accumulate, one might expect that an increased number of nucleation sites would lead to an acceleration of infectivity with exponential kinetics. Such an increase of nucleation sites could result from a branching pattern of polymerization or from fragmentation of aggregates. Breakage could occur if a

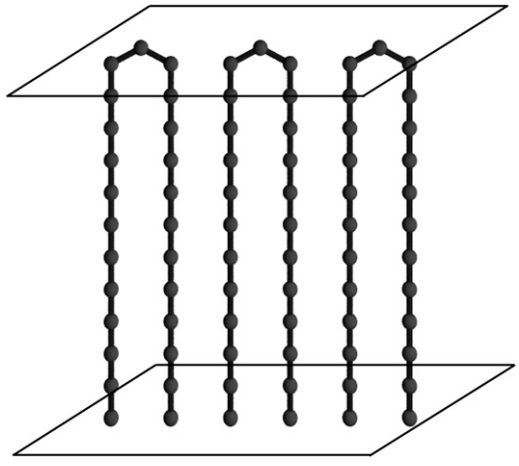

FIGURE 6 Structures of model amyloid protofibrils obtained in simulations of three molecules.

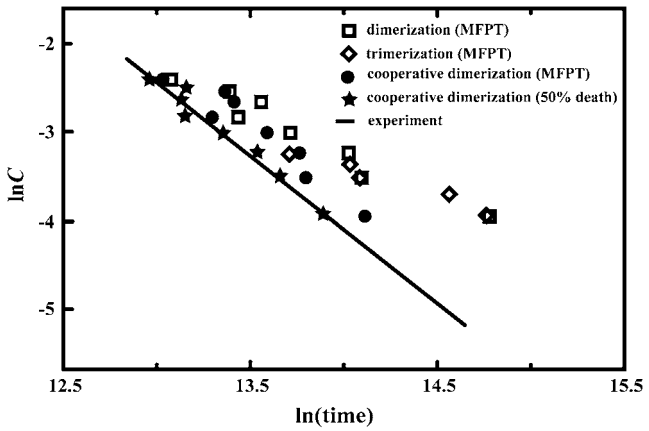

FIGURE 7 Comparison of the correlation curves between MFPT and the concentration (C) of misfolded prions for dimerization (*open squares*), trimerization (*open diamonds*), cooperative dimerization (*solid circles*, MFPT; *solid stars*, 50% death rate), and experimental results from Prusiner et al. (25).

β-form within a fibril makes a rare transition to the helix form. Nevertheless, intensive computer simulations of the exponential kinetics at our resolution are quite difficult based on our current computing facilities. A more coarse-grained approach might be more appropriate to study this problem (37). In the lag phase, our assumption is that each misfolded prion protein nucleates to form a stable amyloid oligomer by either dimerization or trimerization. The doubling phase follows after amyloid oligomers grow to their fission dimension. For our computer simulations of dimerization and trimerization, we observe similar power law dependence between the concentration of misfolded prions and MFPT. However, their exponents are $\gg -1.6$ (-0.9 for dimerization and -0.6 for trimerization). Such a discrepancy indicates that these two processes are too slow to initiate prion disease at low concentrations. It will take a much longer time for those mice to develop signs of prion disease in these two processes.

Previous studies have suggested several sources of cooperative effect in the formation of β-hairpins. It has been found that both hydrogen-bonding pattern and special side-chain packing arrangement can provide cooperative stabilization of strand-strand association in hairpin formation (38–40). It is also observed that orientational order and lateral density fluctuations of the lipid matrix can enhance spontaneous formation of hairpins for some membrane proteins (41,42). Therefore we believe that the cooperative effect may play an important role in the formation of prion oligomers. Computer simulations of cooperativity-enhanced dimerization are performed by biasing the preference in forming hydrogen-bonding pairs of the TM domain. That is, if the motion of a residue leads to the formation of a hydrogen-bonding pair consistent with other hydrogen-bonding pairs in the template, we add an extra favorable factor $\exp(\beta\Delta h)$ in the moving probability of this residue to enhance the cooperative hairpin formation (without violating the detail balance), where Δh is the change in the number of hydrogen-bonding pairs consistent with hydrogen-bonding pairs in the template and β is the cooperative factor (26). In other words, there is a bias in the energy of hydrogen-bonding pairs depending on their orientation. As shown in Fig. 8, it is found that the MFPT of cooperative dimerization is minimized at $\beta = 0.001$. Since the cooperative effect is sequence-dependent, we assume that the cooperative factor of the TM sequence discussed above is at the optimal value. The cumulative distribution of first passage time of cooperative dimerization is shown in Fig. 9 for $C = 4.04\%$ (*dashed line*) and 9.15% (*solid line*), which shows a considerably broader cumulative distribution at low concentrations as suggested in previous studies (37,43). It is clear that the damage or death of neurons due to the aggregation of transmembrane prions occur throughout the incubation period. It is plausible to assume that transgenic mice might enter the doubling phase and quickly develop clinical signs of neurological dysfunction after cumulative death (or cumulative aggregation of amyloid oligomers to their fission dimension) of initially infected neurons reaches a critical value (which we assume to be 50% of initially infected neurons), since neuronal death could further enhance the fission of the transmembrane amyloids. The relationship between concentration and the time for 50% death rate is also illustrated in Fig. 7. The correlation curves (*solid circles* for MFPT and *solid stars* for time of 50% death rate) between folding time and the concentration of misfolded PrP for this cooperative dimerization are compared to the experimental correlation curve in Fig. 7, showing an excellent agreement between our simulations and the experiment. The scaling exponent of the cooperative dimerization is -1.5 for the curve of MFPT and is -1.6 for the curve of 50% death rate, whose values are almost the same as the experimental scaling exponent -1.6. Assuming a different critical value of death rate (40% and 60%) only changes our results slightly. This exponent is obtained from our model in a parameter-free

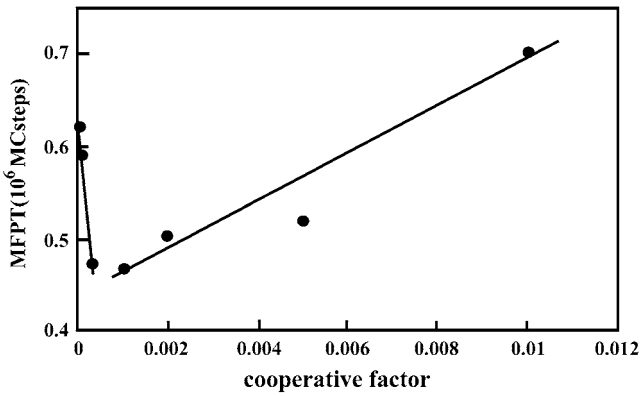

FIGURE 8 The β-dependence of MFPT for a cooperative dimerization of the amino-acid sequence HMAGAAAAGA VVGGLGGYML GSAMV. The initial configuration includes a β-hairpin template and a free α-helical motif.

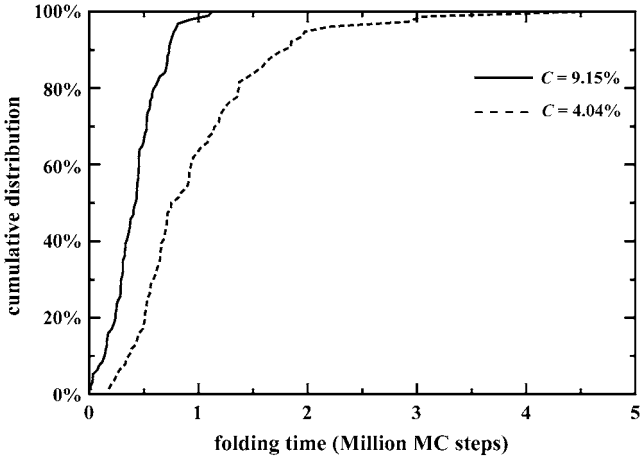

FIGURE 9 Cumulative distribution of the first passage time for cooperative dimerization at $C = 4.04\%$ and 9.15%. One hundred different computer simulations are carried out for each concentration.

manner. The energy parameters are chosen to insure that the unique ground state is a transmembrane helix for a single protein system but is a linear hairpin aggregation for a multiprotein system. The degree of cooperativity is chosen to be its optimal value. There is no free parameter to tune to fit the experimental exponent.

Note that we have assumed that the prion sequence considered in this study has an optimal cooperative factor to facilitate the propagation of β-hairpins. If a different sequence is considered, its cooperative factor could deviate from the optimal value and the formation of β-hairpins would be considerably slowed down. Moreover, other mutated sequences would have different thermodynamic distribution of three topological forms of PrP, and only overexpressing the transmembrane form ^{Ctm}PrP has been shown to be able to develop a spontaneous neurological disease with scrapie-like features in some prion diseases such as Gerstmann-Straussler-Scheinker disease. Thus although the energy function of this model does not distinguish the difference among various hydrophobic transmembrane sequences, the proposed propagation of β-hairpins in the membrane would occur only when the sequence has an optimal cooperative factor and its transmembrane ^{Ctm}PrP dominates the PrP distribution. Nevertheless, the complexity to study sequence-dependent cooperative factor and thermodynamic distribution of various topological forms of PrP would require detailed information of proteins at the atomic level and beyond the scope of our coarse-grained model.

CONCLUSION

In conclusion, we have proposed in this article a possible mechanism for prion diseases based on previous experimental findings. Our model assumes that aggregation of the β-form TM domain of ^{Ctm}PrP is responsible for the development of these neurodegenerative diseases. We speculate that the amyloid aggregation in the membrane could lead to membrane rupture and cause the death of nerve cells. Based on computer simulations, we have investigated the correlation between folding time and the concentration of misfolded PrP in various processes, including dimerization, trimerization, and cooperative dimerization, and compared them with the experimental correlation curve between incubation time and injected dose of Sc237 prions. The exponent of experimental curve is the same as that calculated from our model, which has no free parameter to tune to fit the experimental value. We conclude that cooperativity-enhanced dimerization may play an important role in the pathological mechanism of prion diseases.

We acknowledge partial support by the National Science Council of Taiwan under grant No. NSC 94-2112-M-003-012.

REFERENCES

1. Prusiner, S. B. 1998. Prions. *Proc. Natl. Acad. Sci. USA*. 95:13363–13383.
2. Weissmann, C. 1999. Molecular genetics of transmissible spongiform encephalopathies. *J. Biol. Chem.* 274:3–6.
3. Johnson, R. T., and C. J. Gibbs. 1998. Creutzfeldt-Jakob disease and related transmissible spongiform encephalopathies. *N. Engl. J. Med.* 399:1994–2004.
4. Horwich, A. L., and J. S. Weissman. 1997. Deadly conformations—protein misfolding in prion disease. *Cell.* 89:499–510.
5. Weissmann, C. 2004. The state of the prion. *Nat. Rev. Microbiol.* 2: 861–871.
6. Manson, J. C., A. R. Clarke, P. A. McBride, I. McConnell, and J. Hope. 1994. PrP gene dosage determines the timing but not the final intensity or distribution of lesions in scrapie pathology. *J. Neurodeg.* 3:331–340.
7. Bûeler, H., A. Raeber, A. Sailer, M. Fischer, A. Aguzzi, and C. Weissmann. 1994. High prion and PrP^{Sc} levels but delayed onset of disease in scrapie-inoculated mice heterozygous for a disrupted PrP gene. *Mol. Med.* 1:19–30.
8. Tateishi, J., K. Koh-ura, T. Kitamoto, C. Tranchant, G. Steinmetz, J. M. Warter, and J. W. Boellaard. 1992. Prion protein gene analysis and transmission studies of Creutzfeldt-Jakob disease. *In* Prion Diseases of Humans and Animals. S. B. Prusiner, J. Collinge, J. Powell, and B. Anderton, editors. Horwood, London.
9. Collinge, J., M. S. Palmer, K. C. Sidle, I. Gowland, R. Medori, J. Ironside, and P. Lantos. 1995. Transmission of fatal familial insomnia to laboratory animals. *Lancet*. 346:569–570.
10. Tateishi, J., P. Brown, T. Kitamoto, Z. M. Hoque, R. Roos, R. Wollman, L. Cervenakova, and D. C. Gajdusek. 1995. First experimental transmission of fatal familial insomnia. *Nature*. 376:434–435.
11. Hayward, P. A., J. E. Bell, and J. W. Ironside. 1994. Prion protein immunocytochemistry: reliable protocols for the investigation of Creutzfeldt-Jakob disease. *Neuropathol. Appl. Neurobiol.* 20:375–383.
12. Hsiao, K. K., D. Groth, M. Scott, S.-L. Yang, H. Serban, D. Rapp, D. Foster, M. Torchia, S. J. DeArmond, and S. B. Prusiner. 1994. Serial transmission in rodents of neurodegeneration from transgenic mice expressing mutant prion protein. *Proc. Natl. Acad. Sci. USA*. 91:9126–9130.
13. Hay, B., R. A. Barry, I. Lieberburg, S. B. Prusiner, and V. R. Lingappa. 1987. Biogenesis and transmembrane orientation of the cellular isoform of the scrapie prion protein. *Mol. Cell. Biol.* 7:914–920.
14. Yost, C. S., C. D. Lopez, S. B. Prusiner, R. M. Myers, and V. R. Lingappa. 1990. Non-hydrophobic extracytoplasmic determinant of stop transfer in the prion protein. *Nature*. 343:669–672.

15. Lopez, C. D., C. S. Yost, S. B. Prusiner, R. M. Myers, and V. R. Lingappa. 1990. Unusual topogenic sequence directs prion protein biogenesis. *Science*. 248:226–229.

16. Hegde, R. S., J. A. Mastrianni, M. R. Scott, K. A. DeFea, P. Tremblay, M. Torchia, S. J. DeArmond, S. B. Prusiner, and V. R. Lingappa. 1998. A transmembrane form of the prion protein in neurodegenerative disease. *Science*. 279:827–834.

17. Hegde, R. S., P. Tremblay, D. Groth, S. J. DeArmond, S. B. Prusiner, and V. R. Lingappa. 1999. Transmissible and genetic prion diseases share a common pathway of neurodegeneration. *Nature*. 402:822–826.

18. Thirumalai, D., D. K. Klimov, and R. I. Dima. 2003. Emerging ideas on the molecular basis of protein and peptide aggregation. *Curr. Opin. Struct. Biol.* 13:146–159.

19. Armen, R. S., M. L. DeMarco, D. O. V. Alonso, and V. Daggett. 2004. Pauling and Corey's α-pleated sheet structure may define the prefibrillar amyloidogenic intermediate in amyloid disease. *Proc. Natl. Acad. Sci. USA*. 101:11622–11627.

20. Malolepsza, E., M. Boniecki, A. Kolinski, and L. Piela. 2005. Theoretical model of prion propagation: a misfolded protein induces misfolding. *Proc. Natl. Acad. Sci. USA*. 102:7835–7840.

21. Harrison, P. M., H. S. Chan, S. B. Prusiner, and F. E. Cohen. 2001. Conformational propagation with prion-like characteristics in a simple model of protein folding. *Protein Sci.* 10:819–835.

22. Slepoy, A., R. R. P. Singh, F. Pázmándi, R. V. Kulkarni, and D. L. Cox. 2001. Statistical mechanics of prion diseases. *Phys. Rev. Lett.* 87:058101.

23. Harrison, P. M., H. S. Chan, S. B. Prusiner, and F. E. Cohen. 1999. Thermodynamics of model prions and its implications for the problem of prion protein folding. *J. Mol. Biol.* 286:593–606.

24. Dima, R. I., and D. Thirumalai. 2002. Exploring protein aggregation and self-propagation using lattice models: Phase diagram and kinetics. *Protein Sci.* 11:1036–1049.

25. Prusiner, S. B., P. Tremblay, J. Safar, M. Torchia, and S. J. DeArmond. 1999. Bioassays of Prions. *In* Prion Biology and Diseases. S. B. Prusiner, editor. Cold Spring Harbor Laboratory Press, Cold Spring Harbor, NY.

26. Chen, C.-M., and C.-C. Chen. 2003. Computer simulations of membrane protein folding: structure and dynamics. *Biophys. J.* 84:1902–1908.

27. Thomas, P. D., and K. A. Dill. 1996. An iterative method for extracting energy-like quantities from protein structures. *Proc. Natl. Acad. Sci. USA*. 93:11628–11633.

28. Hopp, T., and K. Woods. 1981. Prediction of protein antigenic determinants from amino acid sequences. *Proc. Natl. Acad. Sci. USA*. 78:3824–3828.

29. White, S. H., and W. C. Wimley. 1999. Membrane protein folding and stability: physical principles. *Annu. Rev. Biophys. Biomol. Struct.* 28: 319–365.

30. Chen, C.-M. 2001. Lattice model of transmembrane polypeptide folding. *Phys. Rev. E Stat. Nonlin. Soft Matter Phys.* 63:010901.

31. Chen, C.-M., and P. G. Higgs. 1998. Monte-Carlo simulations of polymer crystallization in dilute solution. *J. Chem. Phys.* 108:4305–4314.

32. Tompa, P., G. E. Tusnady, P. Friedrich, and I. Simon. 2002. The role of dimerization in prion replication. *Biophys. J.* 82:1711–1718.

33. Hardy, J., and D. J. Selkoe. 2002. The amyloid hypothesis of Alzheimer's disease: Progress and problems on the road to therapeutics. *Science*. 297:353–356.

34. Kayed, R., E. Head, J. L. Thompson, T. M. McIntire, S. C. Milton, C. W. Cotman, and C. G. Glabe. 2003. Common structure of soluble amyloid oligomers implies common mechanism of pathogenesis. *Science*. 300:486–489.

35. Kimberlin, R. H., and C. A. Walker. 1988. Pathogenesis of experimental scrapie. *In* Novel Infectious Agents and the Central Nervous System. T. Bock and J. Marsh, editors. CIBA Foundation Symposium, Wiley, Chichester.

36. Manuelidis, L., and W. Fritch. 1996. Infectivity and host responses in Creutzfeldt-Jakob disease. *Virology*. 216:46–59.

37. Kulkarni, R. V., A. Slepoy, R. R. P. Singh, D. L. Cox, and F. Pázmándi. 2003. Theoretical modeling of prion disease incubation. *Biophys. J.* 85:707–718.

38. Russell, S. J., T. Blandl, N. J. Skelton, and A. G. Cochran. 2003. Stability of cyclic β-hairpins: asymmetric contributions from side chains of a hydrogen-bonded cross-strand residue pair. *J. Am. Chem. Soc.* 125:388–395.

39. Sharman, G. J., and M. S. Searle. 1998. Cooperative interaction between the three strands of a designed antiparallel β-sheet. *J. Am. Chem. Soc.* 120:5291–5300.

40. Schenck, H. L., and S. H. Gellman. 1998. Use of a designed triple-stranded antiparallel β-sheet to probe β-sheet cooperativity in aqueous solution. *J. Am. Chem. Soc.* 120:4869–4870.

41. Baumgartner, A. 1996. Insertion and hairpin formation of membrane proteins: a Monte Carlo study. *Biophys. J.* 71:1248–1255.

42. Cantor, R. S. 1999. Solute modulation of conformational equilibria in intrinsic membrane proteins: apparent ''cooperativity'' without binding. *Biophys. J.* 77:2643–2647.

43. Mclean, A. R., and C. J. Bostock. 2000. Scrapie infections initiated at varying doses: an analysis of 117 titration experiments. *Philos. Trans. R. Soc. Lond. B Biol. Sci.* 355:1043–1050.